

Unified Text-Image Generation with Weakness-Targeted Post-Training

Jiahui Chen^{1,2*}, Philippe Hansen-Estruch^{1,2}, Xiaochuang Han¹, Yushi Hu¹, Emily Dinan¹, Amita Kamath^{1,3,4}, Michal Drozdal¹, Reyhane Askari-Hemmat¹, Luke Zettlemoyer¹, Marjan Ghazvininejad¹

¹FAIR at Meta, ²University of Texas, Austin, ³University of Washington, ⁴University of California, Los Angeles

*Work done at Meta

Unified multimodal generation architectures that jointly produce text and images have recently emerged as a promising direction for text-to-image (T2I) synthesis. However, many existing systems rely on explicit modality switching, generating reasoning text before switching manually to image generation. This separate, sequential inference process limits cross-modal coupling and prohibits automatic multimodal generation. This work explores post-training to achieve fully unified text-image generation, where models autonomously transition from textual reasoning to visual synthesis within a single inference process. We examine the impact of joint text-image generation on T2I performance and the relative importance of each modality during post-training. We additionally explore different post-training data strategies, showing that a targeted dataset addressing specific limitations achieves superior results compared to broad image-caption corpora or benchmark-aligned data. Using offline, reward-weighted post-training with fully self-generated synthetic data, our approach enables improvements in multimodal image generation across four diverse T2I benchmarks, demonstrating the effectiveness of reward-weighting both modalities and strategically designed post-training data.

Date: January 22, 2026

Correspondence: Jiahui Chen jiahui.k.chen@utexas.edu, Marjan Ghazvininejad ghazvini@meta.com



1 Introduction

Text-to-image (T2I) generation has evolved significantly with the advent of multimodal generative models that output both text and images within a unified architecture Xie et al. (2025); Zhou et al. (2024); Team (2025a). As the field moves toward omni-modal systems that handle multiple modalities simultaneously, a new class of multimodal T2I models has emerged that utilize intermediate text generation to improve image synthesis. Recent multimodal architectures such as BAGEL Deng et al. (2025) exemplify this approach by employing a two-stage inference process: first generating text as an intermediate “reasoning” step, then switching to image generation conditioned on the produced reasoning text. This approach posits that explicit textual reasoning can guide and improve the subsequent image generation process, enabling models to better capture complex semantic relationships and nuanced visual details. However, existing multimodal T2I models often rely on manually controlled modality switching, requiring separate inference calls for text and image generation. This design reveals a core limitation: the model does not intrinsically know when to transition between reasoning and image generation or how to ensure that the generated reasoning text effectively aligns with the resulting image. Consequently, the intermediate text may fail to guide image generation effectively, as evidenced by several benchmarks where BAGEL’s multimodal image generation underperforms its image-only generation Chang et al. (2025); Hu et al. (2024); Lin et al. (2024). These limitations highlight the need for a more integrated approach that can jointly generate text and images in a unified manner, strengthening semantic coupling and enabling seamless cross-modal reasoning.

In this work, we explore whether the T2I performance of multimodal models can be enhanced through post-training to achieve fully unified text-image generation, where text and image tokens are generated within a single inference call rather than distinct, modality-specific stages. In this unified setting, the model autonomously determines when to transition from text reasoning to image synthesis, eliminating the need for separate inference calls and enabling seamless multimodal output. As part of our multimodal post-training process, we investigate the relative importance of each modality during training, assessing whether optimizing both jointly yields greater improvements than focusing on one.

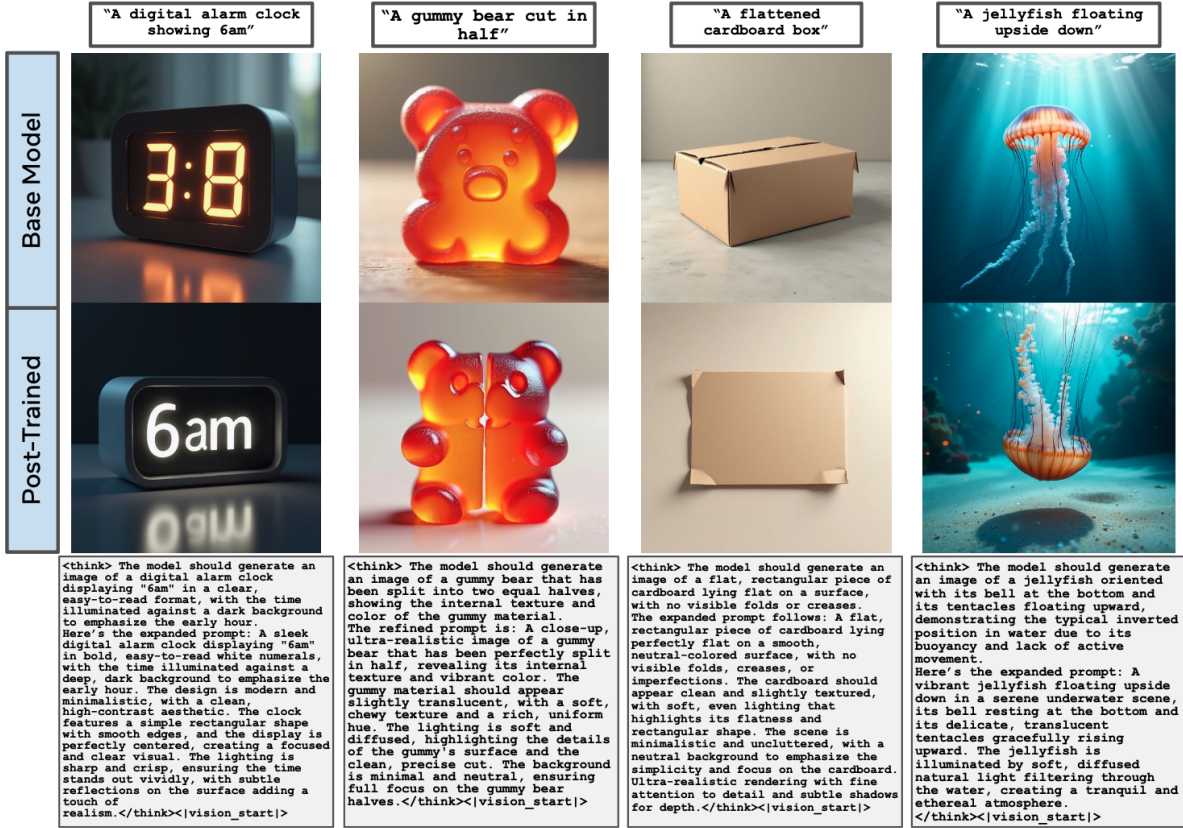


Figure 1 Sample generations before and after our post-training. Our post-training enables successful generations for challenging, previously failed prompts as well as fully automatic joint text-image generation.

Building on the analysis of modality interplay during post-training, we additionally examine how data composition shapes model performance. The prompts used in post-training determine which samples are collected and optimized, making prompt selection a defining factor in model refinement. Existing prompt sourcing strategies vary widely: standard T2I post-training typically relies on broad web-scale image–caption datasets Black et al. (2024); Domingo-Enrich et al. (2025); Xie et al. (2025), while recent online RL methods use benchmark-specific prompts that mirror evaluation sets Liu et al. (2025). Yet, the optimal strategy for selecting prompts remains uncertain. To address this, we systematically compare the standard and benchmark-aligned data strategies with our novel weakness-targeted dataset, showing that tailoring data to model deficiencies yields superior performance over both broad and evaluation-oriented alternatives.

We show that reward-weighting both modalities consistently enhances multimodal image generation performance across four benchmarks with diverse evaluation criteria. Through analysis of T2I reward functions, we identify VQAScore Lin et al. (2024) as the most effective reward and employ an offline reward-weighted regression method that leverages fully self-generated synthetic training data to achieve these performance gains. Central to our approach is a targeted post-training dataset specifically designed to address weaknesses in multimodal models, which we show outperforms both general image-caption pairs and benchmark-derived prompts in improving model capabilities. We hope our findings contribute to more effective training of multimodal models, and we summarize our main contributions below:

- We show that post-training with multimodal reward weighting enables effective joint text–image generation, consistently outperforming other multimodal generation methods across diverse benchmarks. Our approach achieves a 4% gain in object-centric prompt alignment, a 2% improvement in knowledge-based image generation, and a ninefold increase in text rendering accuracy compared to the multimodal baseline.
- We systematically compare post-training data strategies and show that weakness-targeted prompts coupled with the VQAScore reward signal provides the greatest performance gains.

2 Related Work

2.1 Multimodal Generative Models

We define multimodal generative models as systems that process both text and image modalities as inputs and outputs. Existing approaches differ in architecture, influencing their capacity for joint generation and reasoning. **Unified Transformer with Diffusion Components:** share a transformer backbone for both modalities, combining autoregressive (AR) text modeling with diffusion-based image generation; examples include Bagel [Deng et al. \(2025\)](#), Transfusion [Zhou et al. \(2024\)](#), and Show-o [Xie et al. \(2025\)](#). They rely on diffusion [Ho et al. \(2020\)](#) or flow matching [Lipman et al. \(2023\)](#); [Esser et al. \(2024a\)](#) rather than full AR token prediction, limiting seamless interleaving without explicit task tokens. **Fully Autoregressive Models:** generate vision and language tokens within a single AR stream. Janus-Pro [Chen et al. \(2025b\)](#) and Chameleon Team [\(2025a\)](#) encode images as discrete tokens in the same vocabulary as text, enabling unified multimodal generation, while UniGen [Tian et al. \(2025\)](#) adopts a hybrid approach using MaskGIT-style parallel decoding. **Hybrid Pipelines:** pair an AR language model with a separate diffusion or de-tokenization module for image synthesis; BLIP3-o [Chen et al. \(2025a\)](#) first produces image embeddings then decodes them with a diffusion transformer, and SEED-X [Ge et al. \(2025\)](#) generates learnable embeddings decoded by a visual module. These designs achieve high visual quality but remain non-unified and block end-to-end multimodal gradient flow.

2.2 Multimodal Reasoning for T2I Generation

A key goal of multimodal models is leveraging textual reasoning to enhance text-to-image (T2I) synthesis, often by generating intermediate text artifacts or performing self-evaluation during inference. Some methods use vision–language reasoning for self-correction. For example, UniGen [Tian et al. \(2025\)](#) employs a self-verification mechanism where the model generates multiple image candidates, performs VQA-style analyses to assess prompt alignment, and selects the best result through best-of- n filtering. Other work explores interleaved generation of text and images. Interleaving Reasoning Generation (IRG) [Huang et al. \(2025\)](#) iteratively refines outputs by switching between textual reasoning and image synthesis. Such reasoning-driven pipelines improve visual quality and semantic fidelity over prompt-only baselines, though fully integrating reasoning into unified multimodal generators remains an open challenge.

3 Methodology

Our base model, BAGEL [Deng et al. \(2025\)](#), is a 14B-parameter Mixture-of-Transformers (MoT) [Liang et al. \(2025\)](#) architecture that utilizes flow matching for image generation. Online RL incurs substantial computational cost, as each denoising timestep of image generation requires a full MoT forward pass. We therefore adopt reward-weighted regression (RWR) [Peters and Schaal \(2007\)](#) for post-training, weighting the training loss by the sample reward (Section 3.1). Inspired by online RL’s use of sampling for exploration, we use text and image samples from the base model as our training data. To target post-training where it matters, we identify systematic visual patterns that consistently cause failed generations and then create a weakness-targeted training prompt set; we present our analysis of high-failure generation categories in Section 3.2 and demonstrate the effectiveness of training on our dataset in Section 5. Finally, we evaluate a suite of reward functions for their ability to differentiate successful from failed generations, for the effective reward-labelling of our dataset (Section 3.3).

3.1 Reward Weighted Regression For Fully Unified Multimodal Training

We enable fully unified text-image generation by learning the <|vision_start|> token during post-training. At inference time, when <|vision_start|> is generated the model seamlessly switches to image generation mode and conditions the image generation on all of its existing context. Our training data consists of text reasoning traces followed by the <|vision_start|> token and an image. All text and vision tokens are processed as a packed sequence with gradient updates every 50k tokens; full training details are in Appendix C.

For reward-weighted regression (RWR), we extend BAGEL’s original objective by applying an exponentiated reward weight $w_{\text{RWR}}(x_0, c) = \exp(\beta r(x_0, c))$, where $r(x_0, c)$ is the reward for training sample x_0 and prompt c , following prior work [Black et al. \(2024\)](#); [Lee et al. \(2023\)](#). β is the temperature controlling the strength

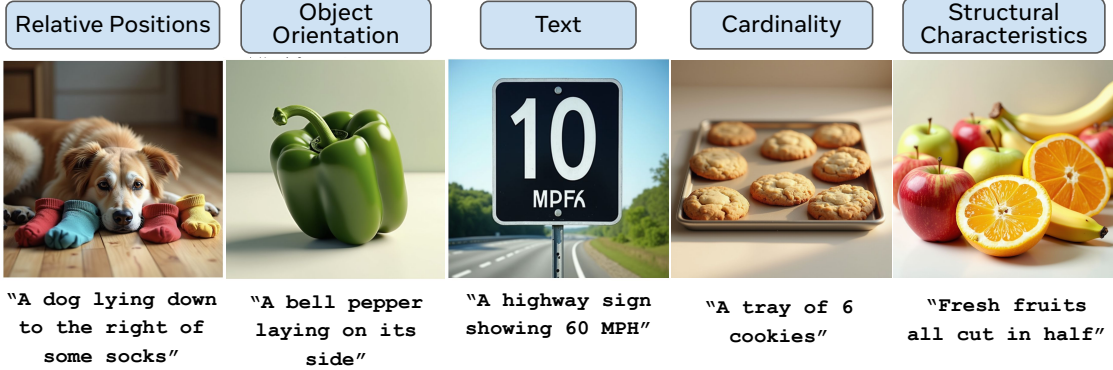


Figure 2 The Multi-Modal Generative Weaknesses (MMGW) Dataset includes five semantic categories that reliably induce generation failures in unified multimodal models. Here we show one representative prompt and failure image for each category.

of the exponential weighting; we use $\beta = 5.0$ and normalize rewards across all samples. Although we also tested rejection sampling, i.e. training only on samples exceeding a reward threshold, RWR outperformed it. BAGEL optimizes MSE loss on image tokens and CE loss on text tokens, allowing reward-weighting of either or both objectives to study modality-specific learning effects (Section 4). We use a single round of sampling, reward labeling, and RWR training, but in general this approach can be repeated for multiple rounds of alternating sampling and training to enable online RL.

3.2 Multi-Modal Generative Weaknesses (MMGW) Dataset

Our base model, BAGEL [Deng et al. \(2025\)](#), is capable of generating samples with high visual quality, making the selection of effective post-training data non-trivial. Unlike standard approaches that rely on broad image-caption datasets, we adopt a targeted strategy, identifying prompts that elicit inconsistent generation quality from the base model, where only a subset of sampled outputs are successful. The intuition is that isolating prompts with high variance in generation quality, then post-training on many synthetic samples with appropriate reward weighting, will enable the model to learn to consistently produce successful generations. This process could easily be automated by generating prompts and evaluating reward intra-prompt reward distributions to find prompts producing high-variance reward distributions.

Since BAGEL’s visual understanding tower, consisting of a pretrained LLM backbone connected to the SigLIP2 [Tschannen et al. \(2025\)](#) vision encoder, predicts the velocity term for flow matching at each image generation timestep, its visual understanding limitations likely translate into image generation weaknesses. We therefore construct our training prompt set from categories known to challenge vision-language models in understanding tasks. The MMVP Benchmark [Tong et al. \(2024\)](#) identifies 9 visual patterns that vision-language models struggle to interpret. We use these patterns along with image captions from MMVP to construct prompts that, through manual testing, result in failed generations approximately 50% of the time—even when using proprietary multimodal generative models like GPT-4o.

We find five semantic categories that consistently cause failed generations: Relative Positions, Object Orientation, Text, Cardinality, and Structural Characteristics, with example failures shown in Figure 2. We call this prompt set the Multi-Modal Generative Weaknesses (MMGW) Dataset. Using approximately 50 manually verified failure-inducing prompts per category (provided in Appendix A) as examples, we use Llama-3-70B-Instruct [AI@Meta \(2024\)](#) to generate 1,000 prompts for the Text category and 500 prompts for each of the other categories, resulting in a final dataset of around 3,500 prompts. For each prompt, we generate 100 samples of both text reasoning traces and images as our training data. However, to effectively leverage this synthetic data for post-training, we must distinguish which samples represent successful generations versus failures—a challenge we address through reward modeling.

3.3 Effective Reward-Labelling of Self-Generated Synthetic Data

We require reward functions capable of distinguishing high-quality from low-quality images, assigning higher rewards to successful generations and lower rewards to failed outputs. Given that our synthetic dataset contains multiple image samples per training prompt, intra-prompt reward variance is essential to enable exploration and differentiate between successful and unsuccessful prompt depictions.

We leverage several existing image reward models: PICKSCORE [Kirstain et al. \(2023\)](#), trained on human-annotated image judgments for producing a score capturing both visual quality and prompt alignment; AESTHETICSCORE [Schuhmann \(2022\)](#), using the LAION aesthetics predictor to evaluate image aesthetic quality; IMAGEREWARD [Xu et al. \(2023\)](#), a human preference reward model capturing text-image alignment, visual fidelity, and harmlessness; and CLIPSCORE [Hessel et al. \(2022\)](#), measuring CLIP embedding similarity between prompts and images as prompt alignment. We also formulate two reward functions utilizing existing work. JPEGSCORE, is defined as the size of the image after JPEG compression, serving as a measure of incompressibility where higher scores indicate greater complexity [Black et al. \(2024\)](#). QWENVQASCORE computes the mean probability of the token “yes” from Qwen2.5-VL-7B-Instruct [Team \(2025b\)](#) when queried with an ensemble of templates similar to: “Does this image match the following text prompt? $\langle p \rangle$ ”, where $\langle p \rangle$ is the target image generation prompt. This approach adapts VQAScore [Lin et al. \(2024\)](#), originally proposed as a prompt alignment evaluation metric.

In Figure 3 we visualize the global reward distributions for all six reward functions across all samples in our MMGW dataset. A key observation is that QwenVQAScore exhibits a bimodal distribution with distinct high-density regions at the extrema (near 0.0 and 1.0), enabling effective discrimination between high-quality and low-quality samples. Analyzing per-prompt reward distributions (Figure 4, Appendix E) shows that QwenVQAScore provides informative reward labels for samples of the same prompt, while other metrics fail to correlate meaningfully with generation quality. Both the global and intra-prompt reward distribution analysis indicate that QwenVQAScore is a valuable reward for training, as it provides a strong learning signal to distinguish successful generations from failures. In contrast, ImageReward, PickScore, ClipScore, AestheticScore, and JPEGScore exhibit unimodal distributions with limited variance, resulting in minimal discriminative power across samples and weak learning signals during training. Consequently, all subsequent experiments use QwenVQAScore as the reward function, with ImageReward results reported in Appendix D for comparison, confirming that QwenVQAScore enables more effective post-training.

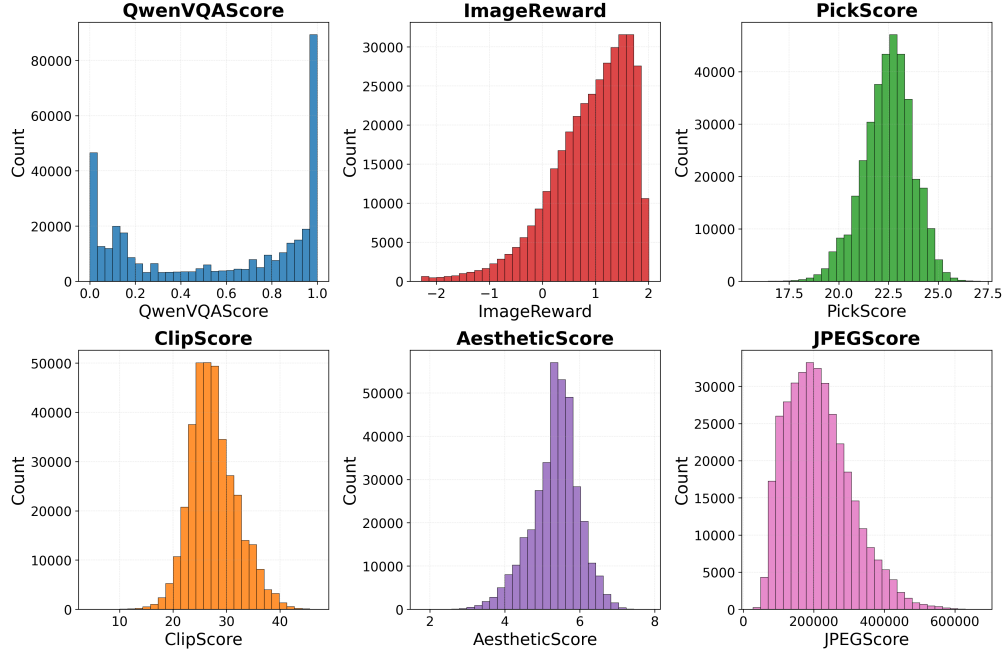


Figure 3 Reward distributions across all samples. QwenVQAScore exhibits a distinct bimodal distribution, effectively discriminating between low-quality and high-quality samples. In contrast, all other reward functions display unimodal distributions with limited variance, resulting in minimal discriminative power across samples.

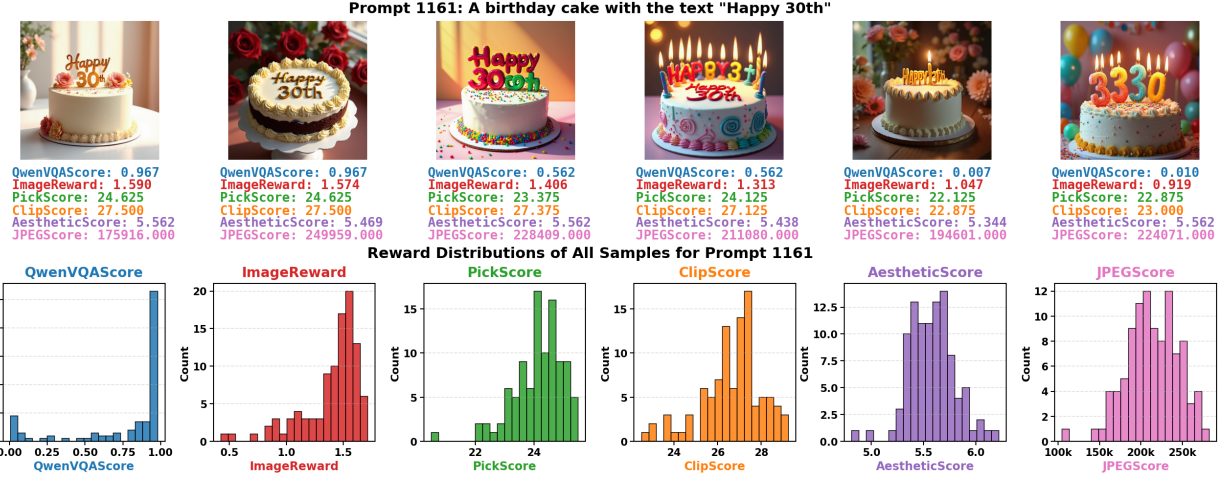


Figure 4 Reward distributions for individual prompts show that QwenVQAScore effectively scores generations and produces intra-prompt rewards that distinguish good from bad samples; more prompt-level reward distributions are shown in Appendix E. Other reward functions do not correlate with generation quality.

4 The Impact of Joint Text-Image Generation on T2I Performance

In this set of experiments, we investigate a key question for unified multimodal generative models: *how much does joint text-image generation contribute to T2I performance?* Intuitively, using a unified model with strong language capabilities to generate text that guides image generation should improve T2I performance. However, multimodal models generally underperform image-only generation models, even on benchmarks requiring implicit knowledge and reasoning [Niu et al. \(2025\)](#); [Wu et al. \(2025\)](#); [Chang et al. \(2025\)](#).

We address this question through systematic modality ablations, comparing multimodal post-training against image-only post-training as well as reward-weighting each modality. Our base model BAGEL is a MoT architecture, enabling selective training or freezing of modality-specific parameters. By training only image-specific parameters versus training both modalities jointly, we isolate and measure the impact of text generation on T2I performance. We additionally compare modality importance in RWR by selectively reward-weighting different loss components: text loss only (Text RWR), image loss only (Image RWR), or both losses jointly (Multimodal RWR). In all RWR runs, parameters for both modalities are trained—only the loss weighting varies across configurations. We train on our MMGW dataset discussed in Section 3.2, with training hyperparameters in Appendix C. All training configurations process the same number of samples for the same number of steps, though the image-only SFT setting trains exclusively on images and omits text traces.

4.1 Quantitative Results

We measure T2I performance across 4 benchmarks: GenEval [Ghosh et al. \(2023\)](#), an object-based prompt alignment benchmark; DPG-Bench [Hu et al. \(2024\)](#), which evaluates prompt alignment on dense prompts; WISE [Niu et al. \(2025\)](#), a benchmark requiring implicit understanding and world knowledge for successful generations; and OneIG-Bench [Chang et al. \(2025\)](#), a very difficult benchmark with fine-grained evaluation spanning prompt-image alignment, text rendering, reasoning-generated content, stylization, and diversity.

As seen in Table 1, Multimodal RWR achieves the best overall performance on GenEval. Multimodal SFT and all other RWR settings slightly improve over BAGEL’s Multimodal performance, but notably Image-Only SFT degrades performance. These results show that multimodal training yields stronger results than image-only training, and reward-weighting both modalities is most effective.

DPG-Bench results in Table 2 show that Multimodal RWR is the best multimodal method, demonstrating a clear improvement over the corresponding BAGEL Multimodal baseline and narrowing the performance gap to the BAGEL Image-Only baseline while outperforming both SFT settings and all existing multimodal models across several subcategories. This suggests that while Image-Only generation remains advantaged on DPG-Bench, reward-weighting both modalities can yield measurable gains.

Table 1 Results on the GenEval Benchmark: The best score is in green and the second-best score in orange. Blue border indicates the best Multimodal score and purple border indicates the best Image-Only score. \dagger denotes base model baseline and $*$ denotes SFT baseline, trained on the same data as RWR but without reward-weighting.

Modality	Ablation	Model	Single Object	Two Object	Counting	Colors	Position	Color Attribute	Overall \uparrow
Image-Only		BAGEL Image-Only \dagger Deng et al. (2025)	0.99	0.93	0.82	0.86	0.52	0.62	0.79
		Image-Only SFT*	0.99	0.91	0.73	0.86	0.45	0.60	0.76
		SD3-Medium Esser et al. (2024b)	0.99	0.94	0.72	0.89	0.33	0.60	0.74
Multimodal		FLUX.1[dev] Labs et al. (2025)	0.98	0.81	0.74	0.79	0.22	0.45	0.66
		Show-o Xie et al. (2025)	0.98	0.80	0.66	0.84	0.31	0.50	0.68
		Janus-Pro-7B Chen et al. (2025b)	0.99	0.89	0.59	0.90	0.79	0.66	0.80
		BAGEL Multimodal \dagger Deng et al. (2025)	0.99	0.94	0.79	0.86	0.50	0.62	0.78
		Multimodal SFT*	0.99	0.93	0.79	0.86	0.54	0.64	0.79
		Text RWR	1.00	0.93	0.79	0.88	0.52	0.60	0.79
		Image RWR	0.99	0.95	0.81	0.91	0.52	0.63	0.80
Overall		Multimodal RWR	0.99	0.97	0.82	0.88	0.61	0.72	0.83

Table 2 Results on the DPG-Bench Benchmark;

Modality	Ablation	Model	Global	Entity	Attribute	Relation	Other	Overall \uparrow
Image-Only		BAGEL Image-Only \dagger Deng et al. (2025)	90.73	90.05	89.72	92.23	90.80	85.08
		Image-Only SFT*	91.59	89.93	89.33	89.97	84.15	83.56
		FLUX.1[dev] Labs et al. (2025)	74.35	90.00	88.96	90.87	88.33	83.84
Multimodal		SD3-Medium Esser et al. (2024b)	87.90	91.01	88.83	80.70	88.68	84.08
		BLIP3-o Chen et al. (2025a)	-	-	-	-	-	81.60
		Janus-Pro-7B Chen et al. (2025b)	86.90	88.90	89.40	89.32	89.48	84.19
		BAGEL Multimodal \dagger Deng et al. (2025)	88.75	90.84	89.01	89.44	89.70	84.01
		Multimodal SFT*	88.73	88.92	88.89	90.04	87.02	83.57
		Text RWR	89.94	89.10	89.24	89.41	90.58	83.84
		Image RWR	90.39	90.87	88.74	87.67	86.97	83.60
Overall		Multimodal RWR	89.20	90.63	89.73	90.03	86.81	84.37

WISE results in Table 3 show Multimodal RWR achieving the best overall score of 0.72. Gains are especially strong in the Chemistry, Physics, and Space categories, indicating that joint reward-weighting of both modalities enhances implicit understanding and factual grounding. Image RWR does not yield improvements over the BAGEL Multimodal baseline and Text RWR slightly degrades performance, indicating that relying solely on uni-modal rewards limits performance. Both Image-Only and Multimodal SFT underperform the BAGEL Multimodal baseline, indicating that synthetic data must be reward-weighted for useful training. These findings suggest that Multimodal RWR provides a balanced and effective signal for improving knowledge-intensive T2I generation.

On OneIG-Bench (Table 4), out of all multimodal methods Multimodal RWR achieves the best Text Rendering score and competitive performance in Reasoning and Style evaluations. It raises the Text score of the BAGEL Multimodal Baseline from 0.020 to 0.189—an approximately ninefold improvement—and improves the Reasoning score from 0.206 to 0.220. Alignment and Style scores remain competitive with BAGEL Multimodal, though Diversity decreases, as expected since RWR post-trains exclusively on synthetic data and up-weights successful samples. Note that OneIG-Bench’s Diversity definition only accounts for embedding space variance of intra-prompt images, with no consideration of prompt alignment or image quality. Relative to Multimodal SFT, all RWR variants improve text rendering—Text RWR 0.057, Image RWR 0.077, and Multimodal RWR 0.189 compared to Multimodal SFT’s 0.010—without sacrificing Alignment or Reasoning performance. Compared to Image-Only SFT, Multimodal RWR also delivers higher Text (0.189 vs 0.046) and better Style (0.370 vs 0.354) score with similar Alignment and Reasoning performance, underscoring the benefits of reward-weighting over standard supervision in unified models. These results show that Multimodal RWR is the most effective configuration among the multimodal runs, improving text rendering while preserving broader capability. Overall on OneIG-Bench, image-only methods outperform

Table 3 Results on the WISE Benchmark Niu et al. (2025); The best score is in green and the second-best score in orange. Blue border indicates the best Multimodal score and indicates the best Image-Only score. \dagger denotes base model baseline and $*$ denotes SFT baseline, trained on the same data as RWR but without reward-weighting.

Modality Ablation	Model	Cultural	Spatio-Temporal		Natural Science			Overall \uparrow
			Time	Space	Biology	Physics	Chemistry	
Image-Only	Image-Only SFT*	0.75	0.67	0.77	0.61	0.74	0.60	0.69
	BAGEL Image-Only \dagger Deng et al. (2025)	0.44	0.55	0.68	0.44	0.60	0.39	0.52
	FLUX.1[dev] Labs et al. (2025)	0.48	0.58	0.62	0.42	0.51	0.35	0.50
	SD3.5 Large Esser et al. (2024b)	0.44	0.50	0.58	0.44	0.52	0.31	0.46
	SD XL Podell et al. (2023)	0.43	0.48	0.47	0.44	0.45	0.27	0.43
Multimodal	BLIP3-o Chen et al. (2025a)	-	-	-	-	-	-	0.62
	T2I-R1 Jiang et al. (2025)	0.56	0.55	0.63	0.54	0.55	0.30	0.54
	Show-o Xie et al. (2025)	0.28	0.40	0.48	0.30	0.46	0.30	0.35
	Janus-Pro-7B Chen et al. (2025b)	0.30	0.37	0.49	0.36	0.42	0.26	0.35
	BAGEL Multimodal \dagger Deng et al. (2025)	0.76	0.69	0.75	0.65	0.75	0.58	0.70
	Multimodal SFT*	0.70	0.64	0.72	0.60	0.77	0.65	0.68
	Text RWR	0.73	0.65	0.75	0.60	0.80	0.63	0.69
	Image RWR	0.73	0.67	0.74	0.64	0.80	0.65	0.70
	Multimodal RWR	0.76	0.69	0.77	0.64	0.77	0.66	0.72

Table 4 Results on the OneIG-Bench Benchmark:

Modality Ablation	Model	Alignment \uparrow	Text \uparrow	Reasoning \uparrow	Style \uparrow	Diversity \uparrow
Image-Only	BAGEL Image-Only \dagger Deng et al. (2025)	0.769	0.244	0.173	0.367	0.251
	Image-Only SFT*	0.798	0.046	0.219	0.354	0.215
	FLUX.1[dev] Labs et al. (2025)	0.786	0.523	0.253	0.368	0.238
	SD XL Podell et al. (2023)	0.688	0.029	0.237	0.332	0.296
	SD3.5 Large Esser et al. (2024b)	0.809	0.629	0.294	0.353	0.225
Multimodal	Show-o Xie et al. (2025)	0.702	0.002	0.213	0.361	0.241
	BLIP3-o Chen et al. (2025a)	0.711	0.013	0.223	0.361	0.229
	Janus-Pro-7B Chen et al. (2025b)	0.553	0.001	0.139	0.276	0.365
	BAGEL Multimodal \dagger Deng et al. (2025)	0.793	0.020	0.206	0.390	0.209
	Multimodal SFT*	0.800	0.010	0.219	0.365	0.143
	Text RWR	0.803	0.057	0.220	0.366	0.149
	Image RWR	0.804	0.077	0.219	0.364	0.144
	Multimodal RWR	0.802	0.189	0.220	0.370	0.141

multimodal, with stark decreases in performance when switching to multimodal generation even when using the same base model, which we discuss in the next section.

4.2 When Multimodal Generation Harms Text-to-Image Performance

The Text category of OneIG-Bench (Table 4) exposes that the performance of Image-Only models is generally much higher than Multimodal models; specifically for BAGEL, Multimodal generation results in a 10x performance degradation compared to Image-Only generation. Multimodal RWR greatly remedies this performance drop, achieving a Text score of 0.189 compared to BAGEL Multimodal’s 0.020, but cannot fully close the gap to BAGEL Image-Only (0.244). These results indicate that text rendering is a specific area in which text-image generation worsens performance compared to image-only generation.

The Text category prompts in OneIG-Bench are highly challenging, requiring generating complex images that accurately render multiple text phrases Chang et al. (2025); figure 5 shows an example prompt and generations. One possible factor behind image-only generation outperforming text-image generation on text rendering tasks is that conditioning on a reasoning trace may overload the model with excessive textual input, as reasoning can guide text placement and scene layout but does not directly improve text rendering. This can be seen in Figure 5, as BAGEL Image-Only’s generation contains the clearest text but a more



Figure 5 Sample generations for a OneIG-Bench Text category prompt. BAGEL Image-Only produces the clearest text, consistent with the stronger text accuracy of image-only generation methods seen in Table 4. Our Multimodal RWR post-training helps remedy some of the text rendering failures of BAGEL Multimodal.

visually cluttered composition compared to the multimodally generated images. Overall these results highlight that although multimodal reward weighting can address some gaps, image-only models still achieve the best performance on certain tasks. This suggests there is still substantial room for improving text-image synergy in unified multimodal frameworks.

5 Post-Training Data Strategies

Our approach uses training prompts from semantic categories that elicit inconsistent generation quality from the base model, where only a subset of samples are successful generations. This contrasts with two common strategies: (1) using general internet-scale image–caption datasets for broad generalization, and (2) employing benchmark-specific prompts that mirror evaluation sets, as in recent online RL work Liu et al. (2025), which optimizes benchmark scores but risks overfitting to the task and prompt design.

To compare these data strategies to our weakness-targeted approach, we run our synthetic data generation and RWR training on three different training prompt sets: (1) captions from a licensed general image-caption dataset; (2) the GenEval-generated prompts from FlowGRPO Liu et al. (2025), constructed using the benchmark’s prompt templates; (3) our MMGW prompt set described in Section 3.2. For all prompt sets, we generate 100 samples of text reasoning and images per prompt and reward-label with QwenVQAScore. All training runs use the best-performing post-training method from Section 4, Multimodal RWR, with the same training settings, and we evaluate performance on the same four benchmarks.

All results are presented in Table 5, with fine-grained results for each benchmark in Appendix B. GenEval Ghosh et al. (2023) results show that while the GenEval-generated dataset predictably improves performance over both the base model and the Shutterstock dataset, our MMGW dataset surprisingly achieves the best performance

Table 5 Results Across All Benchmarks for Data Strategy Ablations: The best score for each benchmark is in **bold green** and the second-best score in *italic orange*.

Training Prompt Set Ablation	GenEval Overall \uparrow	DPG-Bench Overall \uparrow	WISE Overall \uparrow	OneIG-Bench				
				Alignment \uparrow	Text \uparrow	Reasoning \uparrow	Style \uparrow	Diversity \uparrow
Shutterstock	0.79	84.23	0.66	<i>0.801</i>	0.008	<i>0.219</i>	0.369	0.145
GenEval-Generated Liu et al. (2025)	<i>0.82</i>	83.16	<i>0.70</i>	0.797	0.006	0.217	0.358	0.147
MMGW (Ours)	0.83	<i>84.37</i>	0.72	0.802	<i>0.189</i>	0.220	<i>0.370</i>	0.141
BAGEL Multimodal (Baseline) Deng et al. (2025)	0.78	84.01	<i>0.70</i>	0.793	0.020	0.206	0.390	<i>0.209</i>
BAGEL Image-Only (Baseline) Deng et al. (2025)	0.79	85.08	0.52	0.769	0.244	0.173	0.367	0.251

despite not being tailored to GenEval’s specific prompt structure. DPG-Bench [Hu et al. \(2024\)](#) results similarly demonstrate that our MMGW dataset outperforms all other training prompt sets, with Shutterstock also yielding gains over the base model’s multimodal generation. Performance degrades when using GenEval-generated training prompts—an expected outcome given that DPG-Bench’s prompts are approximately four times longer than GenEval’s and contain thousands of unique nouns compared to GenEval’s 80 object classes.

For T2I benchmarks requiring reasoning or world knowledge, our MMGW dataset continues to outperform the other data strategies. On WISE [Niu et al. \(2025\)](#), MMGW enables the best overall T2I performance. Notably, post-training on the Shutterstock dataset causes WISE performance to degrade compared to the base model, indicating that general image-caption prompts may be too simple and out-of-distribution for image generation tasks requiring implicit knowledge integration. On OneIG-Bench [Chang et al. \(2025\)](#), training on MMGW results in the best performance compared to other data strategies on all evaluation axes except for Diversity. MMGW’s targeted prompts notably improve performance on the very difficult Text category, recovering the 10x performance drop of BAGEL’s multimodal generation compared to BAGEL’s image-only generation; whereas all other data strategies result in Text category performance to degrade further.

6 Conclusion and Future Work

In this work, we investigated post-training strategies for fully unified text–image generation, where a model autonomously transitions from textual reasoning to visual synthesis within a single inference process via a learned modality-switch token. Applying Multimodal Reward-Weighted Regression (RWR), which integrates offline reward signals into both text and image losses, improved performance across most benchmarks compared to multimodal baselines. We further find that the choice of post-training data strongly influences outcomes: our weakness-targeted synthetic dataset (MMGW) produces greater improvements than both broad internet-scale image-caption corpora and benchmark-aligned datasets. Combining Multimodal RWR with MMGW achieves the best results among unified multimodal baselines across four diverse T2I benchmarks: GenEval, DPG-Bench, WISE, and OneIG-Bench—including a ninefold gain in text rendering on OneIG-Bench and top performance on the knowledge-intensive WISE benchmark. Finally, our ablations show that standard supervised fine-tuning on synthetic data alone is insufficient and can degrade performance, underscoring the importance of reward-weighting for effective post-training.

Future Work As shown in Section 4.2, image-only generation currently outperforms multimodal generation on text rendering tasks. While our approach narrows the performance gap with image-only models, we see that unified text–image generation is not yet fully competitive. Understanding and bridging this gap remains an important direction for advancing multimodal generation. In particular, exploring how to more effectively leverage joint text–image generation for improving text-to-image (T2I) performance presents several promising research avenues. A detailed analysis of when joint text–image generation helps or hinders T2I performance, compared to image-only approaches, could reveal key factors and guide future efforts for producing effective text reasoning for T2I. Additionally, post-training multimodal models to adaptively use image-only and joint text–image generation, by learning when reasoning is beneficial and when it is not, offers an exciting direction for leveraging strengths of both approaches.

References

AI@Meta. Llama 3 model card. 2024. https://github.com/meta-llama/llama3/blob/main/MODEL_CARD.md.

Kevin Black, Michael Janner, Yilun Du, Ilya Kostrikov, and Sergey Levine. Training diffusion models with reinforcement learning, 2024. <https://arxiv.org/abs/2305.13301>.

Jingjing Chang, Yixiao Fang, Peng Xing, Shuhan Wu, Wei Cheng, Rui Wang, Xianfang Zeng, Gang Yu, and Hai-Bao Chen. Oneig-bench: Omni-dimensional nuanced evaluation for image generation, 2025. <https://arxiv.org/abs/2506.07977>.

Jiuhai Chen, Zhiyang Xu, Xichen Pan, Yushi Hu, Can Qin, Tom Goldstein, Lifu Huang, Tianyi Zhou, Saining Xie, Silvio Savarese, Le Xue, Caiming Xiong, and Ran Xu. Blip3-o: A family of fully open unified multimodal models-architecture, training and dataset, 2025a. <https://arxiv.org/abs/2505.09568>.

Xiaokang Chen, Zhiyu Wu, Xingchao Liu, Zizheng Pan, Wen Liu, Zhenda Xie, Xingkai Yu, and Chong Ruan. Janus-pro: Unified multimodal understanding and generation with data and model scaling, 2025b. <https://arxiv.org/abs/2501.17811>.

Chaorui Deng, Deyao Zhu, Kunchang Li, Chenhui Gou, Feng Li, Zeyu Wang, Shu Zhong, Weihao Yu, Xiaonan Nie, Ziang Song, Guang Shi, and Haoqi Fan. Emerging properties in unified multimodal pretraining, 2025. <https://arxiv.org/abs/2505.14683>.

Carles Domingo-Enrich, Michal Drozdza, Brian Karrer, and Ricky T. Q. Chen. Adjoint matching: Fine-tuning flow and diffusion generative models with memoryless stochastic optimal control, 2025. <https://arxiv.org/abs/2409.08861>.

Patrick Esser, Sumith Kulal, Andreas Blattmann, Rahim Entezari, Jonas Müller, Harry Saini, Yam Levi, Dominik Lorenz, Axel Sauer, Frederic Boesel, Dustin Podell, Tim Dockhorn, Zion English, Kyle Lacey, Alex Goodwin, Yannik Marek, and Robin Rombach. Scaling rectified flow transformers for high-resolution image synthesis, 2024a. <https://arxiv.org/abs/2403.03206>.

Patrick Esser, Sumith Kulal, Andreas Blattmann, Rahim Entezari, Jonas Müller, Harry Saini, Yam Levi, Dominik Lorenz, Axel Sauer, Frederic Boesel, Dustin Podell, Tim Dockhorn, Zion English, Kyle Lacey, Alex Goodwin, Yannik Marek, and Robin Rombach. Scaling rectified flow transformers for high-resolution image synthesis, 2024b. <https://arxiv.org/abs/2403.03206>.

Yuying Ge, Sijie Zhao, Jinguo Zhu, Yixiao Ge, Kun Yi, Lin Song, Chen Li, Xiaohan Ding, and Ying Shan. Seed-x: Multimodal models with unified multi-granularity comprehension and generation, 2025. <https://arxiv.org/abs/2404.14396>.

Dhruba Ghosh, Hanna Hajishirzi, and Ludwig Schmidt. Geneval: An object-focused framework for evaluating text-to-image alignment, 2023. <https://arxiv.org/abs/2310.11513>.

Jack Hessel, Ari Holtzman, Maxwell Forbes, Ronan Le Bras, and Yejin Choi. Clipscore: A reference-free evaluation metric for image captioning, 2022. <https://arxiv.org/abs/2104.08718>.

Jonathan Ho, Ajay Jain, and Pieter Abbeel. Denoising diffusion probabilistic models, 2020. <https://arxiv.org/abs/2006.11239>.

Xiwei Hu, Rui Wang, Yixiao Fang, Bin Fu, Pei Cheng, and Gang Yu. Ella: Equip diffusion models with llm for enhanced semantic alignment, 2024. <https://arxiv.org/abs/2403.05135>.

Wenxuan Huang, Shuang Chen, Zheyong Xie, Shaosheng Cao, Shixiang Tang, Yufan Shen, Qingyu Yin, Wenbo Hu, Xiaoman Wang, Yuntian Tang, et al. Interleaving reasoning for better text-to-image generation. *arXiv preprint arXiv:2509.06945*, 2025.

Dongzhi Jiang, Ziyu Guo, Renrui Zhang, Zhuofan Zong, Hao Li, Le Zhuo, Shilin Yan, Pheng-Ann Heng, and Hongsheng Li. T2i-r1: Reinforcing image generation with collaborative semantic-level and token-level cot, 2025. <https://arxiv.org/abs/2505.00703>.

Yuval Kirstain, Adam Polyak, Uriel Singer, Shahbuland Matiana, Joe Penna, and Omer Levy. Pick-a-pic: An open dataset of user preferences for text-to-image generation, 2023. <https://arxiv.org/abs/2305.01569>.

Black Forest Labs, Stephen Batifol, Andreas Blattmann, Frederic Boesel, Saksham Consul, Cyril Diagne, Tim Dockhorn, Jack English, Zion English, Patrick Esser, Sumith Kulal, Kyle Lacey, Yam Levi, Cheng Li, Dominik Lorenz, Jonas Müller, Dustin Podell, Robin Rombach, Harry Saini, Axel Sauer, and Luke Smith. Flux.1 kontext: Flow matching for in-context image generation and editing in latent space, 2025. <https://arxiv.org/abs/2506.15742>.

Kimin Lee, Hao Liu, Moonkyung Ryu, Olivia Watkins, Yuqing Du, Craig Boutilier, Pieter Abbeel, Mohammad Ghavamzadeh, and Shixiang Shane Gu. Aligning text-to-image models using human feedback. *arXiv preprint arXiv:2302.12192*, 2023.

Weixin Liang, Lili Yu, Liang Luo, Srinivasan Iyer, Ning Dong, Chunting Zhou, Gargi Ghosh, Mike Lewis, Wen tau Yih, Luke Zettlemoyer, and Xi Victoria Lin. Mixture-of-transformers: A sparse and scalable architecture for multi-modal foundation models, 2025. <https://arxiv.org/abs/2411.04996>.

Zhiqiu Lin, Deepak Pathak, Baiqi Li, Jiayao Li, Xide Xia, Graham Neubig, Pengchuan Zhang, and Deva Ramanan. Evaluating text-to-visual generation with image-to-text generation, 2024. <https://arxiv.org/abs/2404.01291>.

Yaron Lipman, Ricky T. Q. Chen, Heli Ben-Hamu, Maximilian Nickel, and Matt Le. Flow matching for generative modeling, 2023. <https://arxiv.org/abs/2210.02747>.

Jie Liu, Gongye Liu, Jiajun Liang, Yangguang Li, Jiaheng Liu, Xintao Wang, Pengfei Wan, Di Zhang, and Wanli Ouyang. Flow-grpo: Training flow matching models via online rl, 2025. <https://arxiv.org/abs/2505.05470>.

Yuwei Niu, Munan Ning, Mengren Zheng, Weiyang Jin, Bin Lin, Peng Jin, Jiaqi Liao, Chaoran Feng, Kunpeng Ning, Bin Zhu, and Li Yuan. Wise: A world knowledge-informed semantic evaluation for text-to-image generation, 2025. <https://arxiv.org/abs/2503.07265>.

Jan Peters and Stefan Schaal. Reinforcement learning by reward-weighted regression for operational space control. In *Proceedings of the 24th International Conference on Machine Learning*, ICML '07, page 745–750, New York, NY, USA, 2007. Association for Computing Machinery. ISBN 9781595937933. doi: 10.1145/1273496.1273590. <https://doi.org/10.1145/1273496.1273590>.

Dustin Podell, Zion English, Kyle Lacey, Andreas Blattmann, Tim Dockhorn, Jonas Müller, Joe Penna, and Robin Rombach. Sdxl: Improving latent diffusion models for high-resolution image synthesis, 2023. <https://arxiv.org/abs/2307.01952>.

Christoph Schuhmann. Laion-aesthetics, August 2022. <https://laion.ai/blog/laion-aesthetics/>.

Chameleon Team. Chameleon: Mixed-modal early-fusion foundation models, 2025a. <https://arxiv.org/abs/2405.09818>.

Qwen Team. Qwen2.5-v1, January 2025b. <https://qwenlm.github.io/blog/qwen2.5-v1/>.

Rui Tian, Mingfei Gao, Mingze Xu, Jiaming Hu, Jiasen Lu, Zuxuan Wu, Yinfei Yang, and Afshin Dehghan. Unigen: Enhanced training and test-time strategies for unified multimodal understanding and generation, 2025. <https://arxiv.org/abs/2505.14682>.

Shengbang Tong, Zhuang Liu, Yuexiang Zhai, Yi Ma, Yann LeCun, and Saining Xie. Eyes wide shut? exploring the visual shortcomings of multimodal llms, 2024. <https://arxiv.org/abs/2401.06209>.

Michael Tschannen, Alexey Gritsenko, Xiao Wang, Muhammad Ferjad Naeem, Ibrahim Alabdulmohsin, Nikhil Parthasarathy, Talfan Evans, Lucas Beyer, Ye Xia, Basil Mustafa, Olivier Hénaff, Jeremiah Harmsen, Andreas Steiner, and Xiaohua Zhai. Siglip 2: Multilingual vision-language encoders with improved semantic understanding, localization, and dense features, 2025. <https://arxiv.org/abs/2502.14786>.

Chenfei Wu, Jiahao Li, Jingren Zhou, Junyang Lin, Kaiyuan Gao, Kun Yan, Sheng ming Yin, Shuai Bai, Xiao Xu, Yilei Chen, Yuxiang Chen, Zecheng Tang, Zekai Zhang, Zhengyi Wang, An Yang, Bowen Yu, Chen Cheng, Dayiheng Liu, Deqing Li, Hang Zhang, Hao Meng, Hu Wei, Jingyuan Ni, Kai Chen, Kuan Cao, Liang Peng, Lin Qu, Minggang Wu, Peng Wang, Shuting Yu, Tingkun Wen, Wensen Feng, Xiaoxiao Xu, Yi Wang, Yichang Zhang, Yongqiang Zhu, Yujia Wu, Yuxuan Cai, and Zenan Liu. Qwen-image technical report, 2025. <https://arxiv.org/abs/2508.02324>.

Jinheng Xie, Weijia Mao, Zechen Bai, David Junhao Zhang, Weihao Wang, Kevin Qinghong Lin, Yuchao Gu, Zhijie Chen, Zhenheng Yang, and Mike Zheng Shou. Show-o: One single transformer to unify multimodal understanding and generation, 2025. <https://arxiv.org/abs/2408.12528>.

Jiazheng Xu, Xiao Liu, Yuchen Wu, Yuxuan Tong, Qinkai Li, Ming Ding, Jie Tang, and Yuxiao Dong. Imagereward: Learning and evaluating human preferences for text-to-image generation, 2023. <https://arxiv.org/abs/2304.05977>.

Chunting Zhou, Lili Yu, Arun Babu, Kushal Tirumala, Michihiro Yasunaga, Leonid Shamis, Jacob Kahn, Xuezhe Ma, Luke Zettlemoyer, and Omer Levy. Transfusion: Predict the next token and diffuse images with one multi-modal model, 2024. <https://arxiv.org/abs/2408.11039>.

Appendix

A MMGW Dataset Prompt Subset

We provide ~ 50 prompts from each of the 5 categories of our Multi-Modal Generative Weaknesses (MMGW) dataset used in post-training. These prompts were manually verified to yield generation failures in the majority of samples when using leading multimodal generative models, including GPT-4o—and we use them as examples to LLM-generate our full MMGW prompt dataset. Our main paper results show that synthetic datasets generated using MMGW prompts yielded effective post-training gains.

Relative Positions

An orange cat sitting in front of a coffee cup on a table, A cat on top of a bird, A gnome behind a hut, A tropical cocktail on the left of flip-flops on a beach, A dog lying down to the right of some socks, A red apple placed behind a glass of water, A teddy bear sitting to the left of a stack of books, A sponge on top of a bottle of dish soap, A bicycle behind a tree, A pair of sunglasses under a beach towel, A hair clip to the right of a hairbrush, A moose walking to the right of a squirrel, A bird standing at the base of a fountain, A hat under a pile of scarves, A husky resting behind a sled, A horse standing behind a tractor, A herd of sheep behind a barn, Deer behind a campsite, Squirrels behind a picnic table, A book inside a briefcase, A painting resting on the ground below a shelf, A fish swimming behind a rock in an aquarium, Wolves behind a winter cabin, A kite flying to the left of a seagull, Candy scattered outside of an empty jar, Paper towels to the right of dirty dishes, A bird standing on top of a birdhouse, A bar of soap on top of a sink, An elf hiding behind a rock, Eggs outside of an empty carton, A guitar leaning against the left side of a wall, A bunny hiding behind a bush, Milk cartons behind a cat, A clock on the wall under a shelf, A book on a shelf to the right of a globe, A marlin swimming behind a school of fish, A pair of gloves to the right of some boots, A bicycle parked to the left of a lamppost, Clown fish swimming behind a sea anemone, A dolphin jumping out of the water in front of a boat, A herding dog behind of a flock of sheep, A rose growing to the left of a fire hydrant, A picture frame resting on top of a box, Pigs behind a chicken coop, A herd of water buffalo behind a jeep, A turtle basking behind some ducks, A book on a table to the left of a cup of tea, A bow to the right of a pair of heels, A hairbrush hanging in front of a mirror, An ant stuck under an apple, A purse behind a vase of flowers

Object Orientations

A motorcycle lying down, An upside down water bottle, A bell pepper lying on its side, A spider flipped over, A chair turned upside down, A jug of milk knocked over on its side, A spoon resting on its side, A bunch of carrots hanging upside down, A perfume bottle lying flat, A computer monitor knocked over, laying flat, A hat placed upside down, A calculator lying face down, A beetle stuck upside down, A bicycle lying on its side, A mug standing upside down, A plate balanced on its rim, A clock face down on a table, A chair leaning against a wall, A vase lying on its side, A camera placed upside down, A pill bottle standing upside down, A suitcase lying flat, A lamp knocked over on its side, A skateboard flipped over, lying upside down, A basket turned upside down, A picture frame lying flat, A cup standing upside down on its rim, An open book lying face down on its pages, A chair turned on its side, A computer mouse placed upside down, A plate lying face down, A teddy bear lying face down, A fish swimming upside down, A whale swimming up towards the ocean surface, A crab flipped upside down, A daisy lying face down, A ring rolling along its edge, An upside down tomato resting on its stem, A pinneapple lying on its side, A wine glass lying on its side, Roller skates lying flat on their side, A keyboard lying upside down, A jellyfish floating upside down, A television lying flat on its face on the ground, A coin standing up on its edge, An upside down toaster, A stool turned upside down, A turtle flipped over on its shell, A penguin lying flat on its belly, An upside down tissue box, A pair of boots knocked down lying flat

Text

A book page showing a photo of a jaguar swimming with the caption "Jaguars are great swimmers.", An astronaut floating in space has a speech bubble that says "Earth is so small from here", An angry dog frowning and saying "You fed me less today!", A still from a movie scene with the subtitles "It was all in his head.", A minimalistic invitation card that reads "Join us for our destination wedding" with a small palm tree icon., A minimalistic card that reads "Missing you, get well soon!" with a bandaged cat., A movie poster with the title "Zombie Cats" showing menacing cartoon cats, with a subtitle that says "The purr-fect horror comedy!", A gaming poster titled "Galactic Quest" showing a space adventurer with the subtitle "Embark on an interstellar journey.", A children's adventure book titled "Jungle Quest" with explorers and the subtitle "Thrills in the wild.", A large hospital with the name "Houston Medical Complex" is in a busy downtown area, A cozy tavern in a medieval village with a sign that reads "The Drunken Dragon", A highway sign showing 60 MPH, A digital alarm clock showing 6am, A comic book character saying "hello", A magazine cover with the title: Home Interiors, A book cover with the title: "Animals", A billboard showing the words: "Sale", A street sign showing "Missiont St", A restaurant sign with the title "Mary's", A website banner reading "Breaking News", A poster with the words "Live Concert Tonight", A chalkboard with the phrase "Today's Special", A coffee cup with the words "Good Morning", A banner showing "Happy Holidays", A postcard with the message "Wish You Were Here", A namecard with the name "Sally Smith", A price tag with the number "30\$", A book spine with the title "Mystery Novel", A cereal box with the label "Whole Grain", A wine label with the year "2015", A movie ticket with the time "7:00 PM", A greeting card with the words "Happy Birthday", A jar with a label reading "Milk", A label with the text "Flour", A sign with the words "No Parking", A magazine cover titled "World Travel", A banner with the title "Charity Run", A notebook with the word "Journal", A label on a jar reading "Peanut Butter", A road sign with the distance "10 Miles", A book cover with the author "Jane Austen", A menu board with the drink "Latte", A poster with the date "July 4th", A t-shirt with the phrase "Friyay", A classroom whiteboard with "Algebra" written on it, A poster with the text: "Move Fast", A postcard with the location "Paris", A name plate that says "CEO", A baseball cap with the letters "ATL", A book spine showing the author "Mark Twain", A cereal box with the word "Organic", A wine label with the region "Napa Valley", A sign advertising a movie titled "The Titanic", A greeting card with the phrase "Congratulations!", A sign in a store that says "Eggs", A sign with the words "Exit Only", A magazine cover titled "Health and Fitness", A sidewalk sign titled: "Art Exhibition", A soda can with the label "Zest" on it, A neon sign reading "brunch", A label on a jar reading "Honey", A book cover with the title "Adventure Stories"

Cardinality

A beach with 4 palm trees, 5 birds sitting on a power line, 5 trees in an field, A tray of 6 cookies, A box of 6 markers, 5 ducks swimming in a pond, A cup of 3 pens on a desk, 4 geese swimming in a lake, A box of 6 crayons, 4 pencils in a cup, 3 crabs on a coral reef, 6 flowers in a vase, A fruit basket holding 3 peaches, A crate holding 3 watermelons, A poster with 5 hearts on it, 6 fish in an aquarium, An office with 3 plants, 3 slices of pie on a plate, 10 birds flying in formation, A school of 8 fish in the ocean, A bedroom with 2 houseplants, 4 glasses of champagne on a platter, An egg carton holding 6 eggs, A box of 4 soda cans, A herd of 5 bison, A highway with 4 sportscars on it, 4 bowls in a kitchen cupboard, 6 candles on a cake, 4 acorns on a branch, A poster with 8 types of food on it, 6 glasses in a kitchen cupboard, 4 towels in a bathroom, 5 keys on a keyring, A building with 6 windows, A classroom with 4 desks, A herd of 6 sheep, 4 sandwiches in a deli case, A flag with 10 stars, A poster with 5 plants on it, A fruit basket holding 3 bananas, A shelf with 5 candles, A poster showing 5 planes, A village with 5 huts, 3 houseplants in a living room, A stack of 3 pancakes, A trail of 5 ants, 5 stools at a bar, A crate holding 6 tomatoes, A label with 4 stars, A bakery display case containing 4 cupcakes, 6 popsicles in a freezer

Structural Characteristics

Fresh fruits all cut in half, A piece of paper folded in half, A bent knife, A car with a dented door, A deflated tire, A butterfly with its wings closed, A mug with a missing handle, A piece of fabric torn in half, A cracked phone screen, A chair with a missing leg, A warped tabletop, A television broken in half, A faded photograph of a dog, A scratched CD, A crushed, flattened water bottle, A flattened cardboard box, A flattened soda can, A dented shield, A hummingbird with its wings closed, A watermelon sliced in half, A carrot cut in half, A wooden bridge with splinters, A cake cut in half, A book torn in half, A wooden table with big scratches, A scratched couch, A laptop broken in half, A bent needle, A bent paperclip, A cucumber cut in half, A tree branch broken in half, A table with a missing leg, Drywall with a hole in it, Socks turned inside out, A t-shirt torn in half, Celery sliced in half, A pencil snapped in half, A bent fork, Pants turned inside out, An action figure broken in half, A cupcake with no frosting', A scratched painting on a wall, A boat broken in half, A frayed wire, A dented trash can, A gummy bear cut in half, A plastic bag torn in half, A bent nail, A cracked tile, A chair with the legs broken off, A teddy bear missing an arm

B Detailed Results for Data Strategies Experiments in Section 5

Table 6 Results on the GenEval Benchmark; The best score is in green and the second-best score in orange .

Training Prompt Set Ablation	Single Object	Two Object	Counting	Colors	Position	Color Attribute	Overall ↑
Shutterstock	0.99	0.95	0.73	0.91	0.53	0.66	0.79
GenEval-Generated Liu et al. (2025)	0.98	0.95	0.81	0.90	0.62	0.63	0.82
MMGW (Ours)	0.99	0.97	0.82	0.88	0.61	0.72	0.83
BAGEL Multimodal (Baseline) Deng et al. (2025)	0.99	0.94	0.79	0.86	0.50	0.62	0.78
BAGEL Image-Only (Baseline) Deng et al. (2025)	0.99	0.93	0.82	0.86	0.52	0.62	0.79

Table 7 Results on the DPG-Bench Benchmark; The best score is in green and the second-best score in orange .

Training Prompt Set Ablation	Global	Entity	Attribute	Relation	Other	Overall ↑
Shutterstock	91.60	86.81	88.23	91.26	91.87	84.23
GenEval-Generated Liu et al. (2025)	90.36	88.46	88.53	88.31	89.72	83.16
MMGW (Ours)	89.20	90.63	89.73	90.03	86.81	84.37
BAGEL Multimodal (Baseline) Deng et al. (2025)	88.75	90.84	89.01	89.44	89.70	84.01
BAGEL Image-Only (Baseline) Deng et al. (2025)	90.73	90.05	89.72	92.23	90.80	85.08

Table 8 Results on the WISE Benchmark [Niu et al. \(2025\)](#); The best score is in green and the second-best score in orange .

Training Prompt Set Ablation	Cultural	Spatio-Temporal		Natural Science			Overall ↑
		Time	Space	Biology	Physics	Chemistry	
Shutterstock	0.72	0.62	0.69	0.58	0.74	0.62	0.66
GenEval-Generated Liu et al. (2025)	0.71	0.68	0.74	0.63	0.76	0.66	0.70
MMGW (Ours)	0.76	0.69	0.77	0.64	0.77	0.66	0.72
BAGEL Multimodal (Baseline) Deng et al. (2025)	0.76	0.69	0.75	0.65	0.75	0.58	0.70
BAGEL Image-Only (Baseline) Deng et al. (2025)	0.44	0.55	0.68	0.44	0.60	0.39	0.52

Table 9 Results on the OneIG-Bench Benchmark; The best score is in green and the second-best score in orange .

Training Prompt Set Ablation	Alignment ↑	Text ↑	Reasoning ↑	Style ↑	Diversity ↑
Shutterstock	0.801	0.008	0.219	0.369	0.145
GenEval-Generated Liu et al. (2025)	0.797	0.006	0.217	0.358	0.147
MMGW (Ours)	0.802	0.189	0.220	0.370	0.141
BAGEL Multimodal (Baseline) Deng et al. (2025)	0.793	0.020	0.206	0.390	0.209
BAGEL Image-Only (Baseline) Deng et al. (2025)	0.769	0.244	0.173	0.367	0.251

C Training Hyperparameters

Table 10 Training hyperparameters used in all experiments in Sections 4 and 5.

Hyperparameter	Value
Total Training Steps	5500
Warm-Up Steps	1000
Learning Rate (LR)	5×10^{-5}
LR scheduler	Constant
Sequence Length (per rank)	50,000 (Tokens)
Optimizer	AdamW ($\beta_1 = 0.9$, $\beta_2 = 0.95$, $\epsilon = 1.0 \times 10^{-15}$)
Gradient Norm Clip Threshold	1.0
Image Generation Resolution (min short side, max long side)	(512, 512)
Image Understanding Resolution (min short side, max long side)	(224, 518)

D ImageReward for RWR Results

Results using ImageReward [Xu et al. \(2023\)](#) as the reward weight during Reward-Weighted Regression post-training as described in Section 3.1 are presented for GenEval [Lin et al. \(2024\)](#) in Table 11, DPG-Bench [Hu et al. \(2024\)](#) in Table 12, WISE [Niu et al. \(2025\)](#) in Table 12, and OneIG-Bench [Chang et al. \(2025\)](#) in Table 14. Across all benchmarks, QwenVQAScore as the RWR reward weight outperforms ImageReward. Notably on WISE, the knowledge-based image generation benchmark, all three modality weighting applications of ImageReward regress the overall score compared to the BAGEL Multimodal base model; this suggests that ImageReward is an especially low quality reward for T2I tasks that require implicit understanding of world knowledge. These results validate our conclusion from Section 3.3 that, among the six rewards evaluated, QwenVQAScore is the most effective.

Table 11 Results on the GenEval Benchmark; The best score is in green and the second-best score in orange. Blue border indicates the best Multimodal score and purple border indicates the best Image-Only score. \dagger denotes base model baseline and $*$ denotes SFT baseline, trained on the same data as RWR but without reward-weighting.

Modality Ablation	Model	Single Object	Two Object	Counting	Colors	Position	Color Attribute	Overall \uparrow
Image-Only	BAGEL Image-Only \dagger Deng et al. (2025)	0.99	0.93	0.82	0.86	0.52	0.62	0.79
	Image-Only SFT $*$	0.99	0.91	0.73	0.86	0.45	0.60	0.76
	SD3-Medium Esser et al. (2024b)	0.99	0.94	0.72	0.89	0.33	0.60	0.74
	FLUX.1[dev] Labs et al. (2025)	0.98	0.81	0.74	0.79	0.22	0.45	0.66
Multimodal	Show-o Xie et al. (2025)	0.98	0.80	0.66	0.84	0.31	0.50	0.68
	Janus-Pro-7B Chen et al. (2025b)	0.99	0.89	0.59	0.90	0.79	0.66	0.80
	BAGEL Multimodal \dagger Deng et al. (2025)	0.99	0.94	0.79	0.86	0.50	0.62	0.78
	Multimodal SFT $*$	0.99	0.93	0.79	0.86	0.54	0.64	0.79
	Text RWR: QwenVQAScore	1.00	0.93	0.79	0.88	0.52	0.60	0.79
	Text RWR: ImageReward	1.00	0.93	0.75	0.88	0.53	0.63	0.78
	Image RWR: QwenVQAScore	0.99	0.95	0.81	0.91	0.52	0.63	0.80
	Image RWR: ImageReward	0.98	0.93	0.64	0.88	0.53	0.66	0.77
	Multimodal RWR: QwenVQAScore	0.99	0.97	0.82	0.88	0.61	0.72	0.83
	Multimodal RWR: ImageReward	1.0	0.93	0.77	0.87	0.58	0.67	0.80

Table 12 Results on the DPG-Bench Benchmark;

Modality Ablation	Model	Global	Entity	Attribute	Relation	Other	Overall \uparrow
Image-Only	BAGEL Image-Only \dagger Deng et al. (2025)	90.73	90.05	89.72	92.23	90.80	85.08
	Image-Only SFT $*$	91.59	89.93	89.33	89.97	84.15	83.56
	FLUX.1[dev] Labs et al. (2025)	74.35	90.00	88.96	90.87	88.33	83.84
	SD3-Medium Esser et al. (2024b)	87.90	91.01	88.83	80.70	88.68	84.08
Multimodal	BLIP3-o Chen et al. (2025a)	-	-	-	-	-	81.60
	Janus-Pro-7B Chen et al. (2025b)	86.90	88.90	89.40	89.32	89.48	84.19
	BAGEL Multimodal \dagger Deng et al. (2025)	88.75	90.84	89.01	89.44	89.70	84.01
	Multimodal SFT $*$	88.73	88.92	88.89	90.04	87.02	83.57
	Text RWR: QwenVQAScore	89.94	89.10	89.24	89.41	90.58	83.84
	Text RWR: ImageReward	89.71	88.32	88.23	89.89	89.77	83.51
	Image RWR: QwenVQAScore	90.39	90.87	88.74	87.67	86.97	83.60
	Image RWR: ImageReward	85.33	89.70	88.75	89.17	91.22	83.73
	Multimodal RWR: QwenVQAScore	89.20	90.63	89.73	90.03	86.81	84.37
	Multimodal RWR: ImageReward	80.61	88.30	88.74	91.28	87.34	83.18

Table 13 Results on the WISE Benchmark Niu et al. (2025); The best score is in green and the second-best score in orange.

Blue border indicates the best Multimodal score and purple border indicates the best Image-Only score. † denotes base model baseline and * denotes SFT baseline, trained on the same data as RWR but without reward-weighting.

Modality Ablation	Model	Cultural	Spatio-Temporal		Natural Science			Overall ↑
			Time	Space	Biology	Physics	Chemistry	
Image-Only	Image-Only SFT*	0.75	0.67	0.77	0.61	0.74	0.60	0.69
	BAGEL Image-Only† Deng et al. (2025)	0.44	0.55	0.68	0.44	0.60	0.39	0.52
	FLUX.1[dev] Labs et al. (2025)	0.48	0.58	0.62	0.42	0.51	0.35	0.50
	SD3.5 Large Esser et al. (2024b)	0.44	0.50	0.58	0.44	0.52	0.31	0.46
Multimodal	SD XL Podell et al. (2023)	0.43	0.48	0.47	0.44	0.45	0.27	0.43
	BLIP3-o Chen et al. (2025a)	-	-	-	-	-	-	0.62
	T2I-R1 Jiang et al. (2025)	0.56	0.55	0.63	0.54	0.55	0.30	0.54
	Show-o Xie et al. (2025)	0.28	0.40	0.48	0.30	0.46	0.30	0.35
	Janus-Pro-7B Chen et al. (2025b)	0.30	0.37	0.49	0.36	0.42	0.26	0.35
	BAGEL Multimodal† Deng et al. (2025)	0.76	0.69	0.75	0.65	0.75	0.58	0.70
	Multimodal SFT*	0.70	0.64	0.72	0.60	0.77	0.65	0.68
	Text RWR: QwenVQAScore	0.73	0.65	0.75	0.60	0.80	0.63	0.69
	Text RWR: ImageReward	0.71	0.62	0.75	0.58	0.74	0.60	0.67
	Image RWR: QwenVQAScore	0.73	0.67	0.74	0.64	0.80	0.65	0.70
	Image RWR: ImageReward	0.72	0.63	0.72	0.59	0.74	0.62	0.67
	Multimodal RWR: QwenVQAScore	0.76	0.69	0.77	0.64	0.77	0.66	0.72
	Multimodal RWR: ImageReward	0.72	0.65	0.74	0.59	0.76	0.63	0.68

Table 14 Results on the OneIG-Bench Benchmark;

Modality Ablation	Model	Alignment ↑	Text ↑	Reasoning ↑	Style ↑	Diversity ↑
Image-Only	BAGEL Image-Only† Deng et al. (2025)	0.769	0.244	0.173	0.367	0.251
	Image-Only SFT*	0.798	0.046	0.219	0.354	0.215
	FLUX.1[dev] Labs et al. (2025)	0.786	0.523	0.253	0.368	0.238
	SD XL Podell et al. (2023)	0.688	0.029	0.237	0.332	0.296
Multimodal	SD3.5 Large Esser et al. (2024b)	0.809	0.629	0.294	0.353	0.225
	Show-o Xie et al. (2025)	0.702	0.002	0.213	0.361	0.241
	BLIP3-o Chen et al. (2025a)	0.711	0.013	0.223	0.361	0.229
	Janus-Pro-7B Chen et al. (2025b)	0.553	0.001	0.139	0.276	0.365
	BAGEL Multimodal† Deng et al. (2025)	0.793	0.020	0.206	0.390	0.209
	Multimodal SFT*	0.800	0.010	0.219	0.365	0.143
	Text RWR: QwenVQAScore	0.803	0.057	0.220	0.366	0.149
	Text RWR: ImageReward	0.803	0.016	0.220	0.359	0.149
	Image RWR: QwenVQAScore	0.804	0.077	0.219	0.364	0.144
	Image RWR: ImageReward	0.803	0.038	0.217	0.357	0.143
	Multimodal RWR: QwenVQAScore	0.802	0.189	0.220	0.370	0.141
	Multimodal RWR: ImageReward	0.802	0.040	0.217	0.348	0.143

E Additional Intra-Prompt Reward Distributions

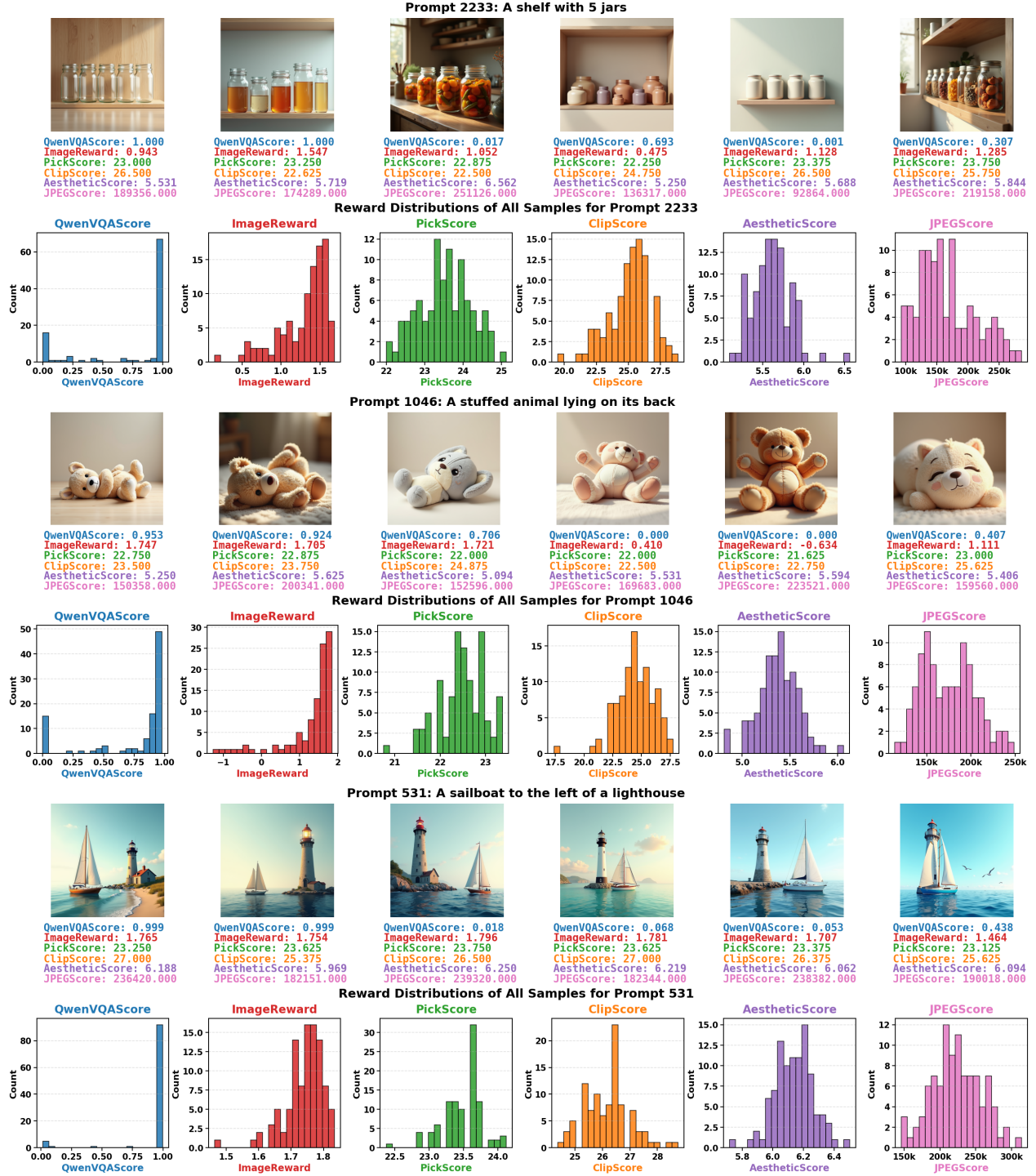


Figure 6 Reward distributions for individual prompts show that QwenVQAScore effectively scores generations and produces intra-prompt rewards that distinguish good from bad samples. Other reward functions do not correlate with generation quality.